

New Matrices and Accelerating Voltage Effects in Matrix-assisted Laser Desorption/Ionization of Synthetic Polymers

Xiaodong Tang,¹ Peter A. Dreifuss² and Akos Vertes^{1*}

¹ Department of Chemistry, The George Washington University, Washington DC 20052, USA

² Washington Research Center, W. R. Grace & Co.-Conn., 7379 Route 32, Columbia, MD 21044, USA

SPONSOR REFEREE: Dr Kevin G. Owens, Drexel University, Philadelphia, PA 19104, USA

Most matrices used in matrix-assisted laser desorption/ionization mass spectrometry (MALDI-MS) have been selected for their sound performance in the detection of proteins. We evaluated a series of new matrices for the analysis of synthetic polymers and compared their performance to that of conventional ones. Among substituted polycyclic aromatic hydrocarbons 1,4-dihydroxy-2-naphthoic acid, 9-anthracenecarboxylic acid (9-ACA), and its mixtures with 5-methoxysalicylic acid ('super' 9-ACA) offered better signal quality for analysis of synthetic polymers. To test the performance of these new matrices, authentic standards of poly(ethylene glycol), poly(propylene glycol), Jeffamine, polybutadiene, poly(methyl methacrylate), poly(dimethyl siloxane), and some of their mixtures were analyzed. By generating mainly $[M + Na]^+$ ions, 9-ACA showed superior performance to most conventional matrices and provided higher effective mass resolution. The 'super' 9-ACA composite matrix was found to be more suitable for larger polymer molecules (>8000 Da).

Broader acceptance of MALDI-MS for synthetic polymer analysis has been delayed by systematic differences observed between MALDI-MS and gel permeation chromatography (GPC) in terms of oligomer size distributions (R. S. Lehrle and D. S. Sarson, *Rapid Commun. Mass Spectrom.*, Vol. 9, p. 91 (1995)). We found that part of the discrepancy can be explained by the profound dependence of mass distributions on the accelerating voltage of the time-of-flight mass spectrometer. With decreasing accelerating voltage both the ion intensity and the mass resolution decreased, and the high-mass end of the mass spectrum became truncated. For example, when the accelerating voltage was changed from 30 kV to 18 kV the center of the peak area distribution for poly(methylmethacrylate) (PMMA) 6000 shifted to lower values by about 210 Da. At the same time, the skewness of the distribution increased tenfold indicating serious discrimination phenomena. These detrimental effects of lower accelerating voltage were particularly strong for relatively large synthetic polymer molecules.

The success of matrix-assisted laser desorption ionization mass spectrometry (MALDI-MS) analysis of biopolymers is known to depend on the choice of the appropriate matrix material.¹ Recently, the use of MALDI-MS has been extended to synthetic polymer analysis.^{2–7} For a number of different synthetic polymers, useful information can be obtained on their number-averaged molecular weight, M_n , weight-averaged molecular weight, M_w , polydispersity, M_w/M_n , repeat unit and end-group masses. Compared to MALDI-MS of proteins, where protonated species with molecular weight up to 300,000 Da can easily be produced, the analysis of synthetic polymers can present challenges even in the 20,000 Da range.

One of the difficulties in the MALDI-MS analysis of synthetic polymers is to find matrices that are miscible with the mostly non-water-soluble polymers. These preferably molecular level mixtures are believed to be prerequisites for successful volatilization during laser desorption. Matrices applied for polar biopolymers, such as sinapinic acid (SA) and 2,5-dihydroxybenzoic acid (DHB), work well with a number of polar polymers, e.g. different fractions of poly(ethylene glycol). In the past 2 years, extensive efforts have been devoted to searching for matrices that can efficiently volatilize and ionize synthetic polymers. Danis and Karr reported the use of trans-3-indoleacrylic acid (IAA) for poly(hydroxystearic acid) and

poly(methylmethacrylate).⁸ Subsequently, Montaudo and co-workers reported that the application of 2-(4-hydroxyphenylazo)-benzoic acid (HABA) matrix substantially enhanced the detection of polystyrene (PS) and poly(butyleneadipate).⁹ In order to facilitate the intimate mixing of matrix and analyte and the cationization process, a host of sample preparation methods have been developed. These include co-crystallization, electrospraying,¹⁰ vacuum drying,¹¹ layering,¹² and mechanical mixing¹³ of the two components. Despite the growing array of matrices and of sample preparation methods, the selection of appropriate conditions for MALDI-MS remains a trial-and-error process.

Although the preliminary MALDI-MS results are quite promising, a systematic discrepancy can often be observed between oligomer size distributions determined by MALDI-MS and the more traditional gel permeation chromatography (GPC).¹⁴ In many cases, the MALDI-MS distributions seem to be shifted to lower mass values. This shift is more pronounced for certain polymers than for others, and seems to increase with increasing average molecular weight.

Searching for more effective matrices of synthetic polymers, we focused our efforts on screening polycyclic aromatic hydrocarbons (PAHs) and their derivatives. These compounds usually have strong absorbance in the UV range and show relatively low sublimation temperatures. In this contribution, we report our performance survey of some matrix candi-

* Author for correspondence.

Table 1. Potential matrix materials for synthetic polymers

Matrix	λ_{\max} (nm) ^a	m.p. (°C)	MALDI response ^b
2-Hydroxy-4-methoxybenzophenone	284, 324 (MeOH)	64	N/A
Naphthalene	266, 276, 284 (EtOH)	81	- (275)
1,4-Dihydroxy-2-naphthoic acid	260, 355 (MeOH)	220	+ (280, 337)
Anthracene	252 (EtOH)	217	- (275)
9-Anthracenecarboxylic acid	254, 344 (EtOH)	220	++ (337)
Phenanthrene	252, 294 (heptane)	101	- (275)
9-Phenanthrol	248, 305, 355 (MeOH)	141	- (275)
<i>o</i> -Phenanthroline	263 (MeOH)	115	- (275)
Pyrene	263, 273, 320, 332 (MeOH)	150	- (275)
Chrysene	269, 295, 307, 321 (MeOH)	254	- (275)
Benzo[a]pyrene	266, 285, 297, 347 (MeOH)	178	- (275)
'Super' 9-ACA	N/A	N/A	++ (337)

^a The solvents, shown in parentheses, were methanol (MeOH), ethanol (EtOH), and heptane.

^b MALDI response was tested with PEG 3300 at the wavelength indicated in parentheses. ++: strong response, +: weak response, -: no response, N/A: not available.

dates in the analysis of synthetic polymers. In order to explain some of the discrepancies between MALDI-MS and GPC data, we examined the effects of accelerating voltage on the observation of oligomer size distributions using rigorous statistical analysis.

EXPERIMENTAL

Instrumentation

All mass spectra were recorded on a home-built linear time-of-flight mass spectrometer (TOF-MS), which has been described in detail previously.¹⁵ Briefly, a nitrogen laser at 337 nm (VSL-337ND, Laser Science Inc., Newton, MA, USA) and an excimer pumped dye laser, tunable between 275 nm and 290 nm (LPD 3000, Lambda Physik, Göttingen, Germany) were used to generate ions from the samples. The ions were extracted by a single-stage acceleration system (maximum 30 kV) into the 2 m field-free drift region of the TOF-MS and detected by a dual microchannel plate (MCP). After $10 \times$ amplification, the signal was sent to a transient recorder (TR8828D, LeCroy, Albuquerque, NM, USA). A custom-made data acquisition package (Toftware, Version 2.1, Ilys Software, Pittsburgh, PA, USA) was utilized to collect and analyze the spectra on a 486 PC. For proteins, a mass resolution of 500 could be routinely achieved at m/z 5000.

Sample preparation

The twelve tested matrix materials, along with their UV absorption maxima, λ_{\max} , melting points and relative MALDI-MS responses are listed in Table 1. For fast screening of the matrix performance we selected PEG 3300 as a relatively 'easy' analyte. The compounds in Table 1 as well as the conventional matrices IAA, SA, sucrose, and 5-methoxysalicylic acid (5-MSA) were purchased from Aldrich Chemical Co. (Milwaukee, WI, USA) and used without purification. DHB was recrystallized three times from water prior to use. 'Super' 9-ACA was prepared as 5:2 molar ratio mixture of 9-ACA and 5-methoxysalicylic acid (5-MSA). We prepared fresh saturated matrix solutions daily in methanol or in 1:1 (v/v) toluene + methanol mixture depending on the polarities of matrix and analyte. All polymer standards were from the American Polymer Standards Co. (Mentor, OH, USA)

and were used as received. The studied polymers included: Poly (ethylene glycol): PEG 610, PEG 3300, PEG 5000, PEG 8000, PEG 10225, PEG 10730, PEG 15000; poly (propylene glycol): PPG 450, PPG 1000, PPG 1200, PPG 2000, PPG 5000; poly (methylmethacrylate): PMMA 2000, PMMA 6000; polybutadiene 1000; Jeffamine 2000; and poly(dimethyl siloxane): PDMS 1500. The certificate of analysis for PMMA 6000 stated that the standard had been analyzed by GPC using American Polymer Standards GPC columns (AM GEL 10³/5, AM GEL 500/5, and AM GEL 100/5) with tetrahydrofuran (THF) eluent at 30 °C. Molecular weight information was based on GPC with differential viscometer detection for M_n and M_w . Vapor-pressure osmometry was also used to obtain M_n values.

The stock solutions of PEG, PPG and Jeffamine were prepared in methanol, while PMMA, polybutadiene and PDMS were dissolved in toluene at 2×10^{-4} M concentrations. Usually 2 μ L polymer sample was mixed with 10 μ L matrix solution in a micro-vial before depositing 10 μ L of the mixture to the probe tip by an Eppendorf pipette. The sample was dried in a stream of ambient air prior to insertion into the mass spectrometer. No salts were added to assist cationization except for polybutadiene 1000. For this analyte 5 μ L silver acetate solution (0.05 M in toluene) was dried onto the probe tip before depositing the matrix/analyte mixture. Substance P (MW 1347.6) and bovine insulin (MW 5733.5) from Sigma Chemical Co. (St. Louis, MO, USA) were used as external standards providing mass accuracy within $\pm 0.1\%$.

Data analysis

Polymer size distributions are usually characterized by the number-averaged molecular weight, M_n , by the weight-averaged molecular weight, M_w , and by the polydispersity, M_w/M_n . In mass spectrometry these values are approximated by the following equations:

$$M_n = \frac{\sum A_i M_i}{\sum A_i} \quad (1)$$

$$M_w = \frac{\sum A_i M_i^2}{\sum A_i M_i} \quad (2)$$

where A_i and M_i represent the detected charge and the molecular weight of the i th oligomer ion, respectively.

To correlate these quantities with expressions used in statistics we refer to the r th momentum, α_r , of a random variable, χ :

$$\alpha_r = \sum_{\chi} \chi^r \rho(\chi) \quad (3)$$

where $\rho(\chi)$ is the probability density of χ . Similarly, the r th central momentum, μ_r , of χ is:

$$\mu_r = \sum_{\chi} (\chi - \xi)^r \rho(\chi) \quad (4)$$

where $\xi = \sum_{\chi} \chi \rho(\chi)$ is the expected value of χ .

Assuming that $\rho(\chi)$ is approximated by $A_i/\sum A_i$, the polymer size distribution can be described by the momenta:

$$M_n = \alpha_1 \quad (5)$$

$$M_w = \frac{\alpha_2}{\alpha_1} \quad (6)$$

$$\text{Polydispersity} = \frac{\alpha_2}{\alpha_1^2} \quad (7)$$

Following the analogy between probability and oligomer size distributions two additional quantities can be utilized to describe their asymmetry and flatness. The skewness, γ_1 , and kurtosis, γ_2 , values are the statistical measures of deviations from symmetry, and flatness or peakedness compared to the normal distribution, respectively. Their definitions are based on the central momenta:

$$\gamma_1 = \frac{\mu_3}{\mu_2^{3/2}} \quad (8)$$

$$\gamma_2 = \frac{\mu_4}{\mu_2^2} - 3 \quad (9)$$

In our analysis, the flight time spectra of 50 consecutive shots were averaged to minimize the shot-to-shot variations and improve the signal-to-noise ratio (S/N). The raw time-dependent ion-current data were evaluated by a scientific graphics package (Origin, MicroCal Software, Inc., Northampton, MA, USA). Baseline corrections relied on averaging dark-current readings in the spectrum outside the area of matrix- and polymer-related peaks. The baseline was established on the basis of finding values that were nearly equal before and after the polymer-related peaks. Thus, the baseline drift could be eliminated. After the baseline subtraction, the area under each oligomer ion current peak, A_i , with $S/N \geq 3$ was determined from the flight-time spectrum. The $S/N \geq 3$ condition was important for establishing the width of a particular peak. At $S/N < 3$, peaks and noise could not be clearly separated; thus the integration boundaries became blurred.

According to the original definition, the $A_i/\sum A_i$ values should correspond to the probability of finding the i th oligomer in the mixture. We approximated A_i with the charge carried by the i th species in the MALDI-MS spectrum. Based on the definitions of current and charge, the charge can be calculated by integrating the ion current, $I(t)$, with respect to time in the TOF spectrum ($Q = \int I(t) dt$). Integrating the mass spectrum, $I(m)$, is an alternative, but requires the transformation of the integrand ($Q = \int I(m) (dt(m)/dm) dm$). Thus, unless one takes into account the $dt(m)/dm$ factor in the integrand the charge values, and consequently the A_i values, will be distorted. The integration method was more accurate

than simply substituting A_i with the height of the peak, especially when low ion intensities were involved. The corresponding M_i values were determined from the calibrated mass spectrum. Based on the A_i and M_i data, α_1 , α_2 , μ_2 , μ_3 , and μ_4 were calculated. Eqs. (5)–(9) were used to express the results in a format more familiar to the polymer chemists. The peak mass (M_p) and centroid mass (M_c) were also estimated from the spectra.

RESULTS AND DISCUSSION

Search for new matrices

The matrix materials were selected on the basis of well established principles: high light absorption coefficient at the laser wavelength, low melting point (sublimation temperature), miscibility with the analyte, and assistance in analyte-ion formation. Because of the non-polar character of many synthetic polymers, we experimented with some truly non-polar polycyclic aromatic hydrocarbons (PAH). MALDI-MS experiments with the six non-substituted PAHs, however, were consistently unsuccessful, as were those with the heterocyclic matrix material (*o*-phenanthroline).

When we turned to PAHs substituted with different polar groups, we experienced varying degrees of success. The 2-hydroxy-4-methoxybenzophenone-based samples underwent vigorous sublimation in the vacuum system. After sample loading, by the time the mass spectrometer reached operating pressure, the matrix had completely sublimed from the probe. 1,4-dihydroxy-2-naphthoic acid (DHNA) worked very well at 280 nm and 337 nm wavelengths, especially with non-polar polymers (e.g. polystyrene). Among the four substituted PAHs, 9-ACA turned out to be the most universally effective by far. We compared the performance of 9-ACA to previously described matrices like IAA and DHB.

One of the problems in MALDI-MS of polymers had been the presence of both Na^+ and K^+ adduct ions. Ion exchange has been used to get rid of both alkaline ions, followed by doping with Na^+ alone.¹⁶ In contrast to the conventional matrices, 9-ACA produced a uniform series of Na^+ adduct polymer ions. We were able to eliminate sample pretreatment, i.e. purification by ion-exchange or addition of cation salts to get a more homogeneous cationization. Better quality spectra with 9-ACA are perhaps related to the lower level of alkaline contaminants in this matrix material. The purity of matrix materials is only guaranteed to be better than 98% by the manufacturer (Aldrich Chemical Co.). In many cases the remaining 2% is composed of alkaline salts. For example, since DHB was known to be contaminated by sodium salts we used triply recrystallized DHB for MALDI experiments. An advantage of using 9-ACA was the ease of finding a "sweet" spot on the probe that survived tens, even hundreds of laser shots before the analyte signal decayed.

The performance of 9-ACA and IAA is compared for a polymer standard (PEG 3300) in Fig. 1. For both matrices intense oligomer ions ranging from m/z 2300 to 4300 were observed and the corresponding molecular weight distributions were characterized by $M_n \approx 3324$, $M_w \approx 3360$ for IAA and $M_n \approx 3288$, $M_w \approx 3330$ for 9-ACA. Two series of peaks were observed in IAA matrix, originating from Na^+ and K^+ adducts. The intensity of $[\text{M} + \text{K}]^+$ was over 70% of that of

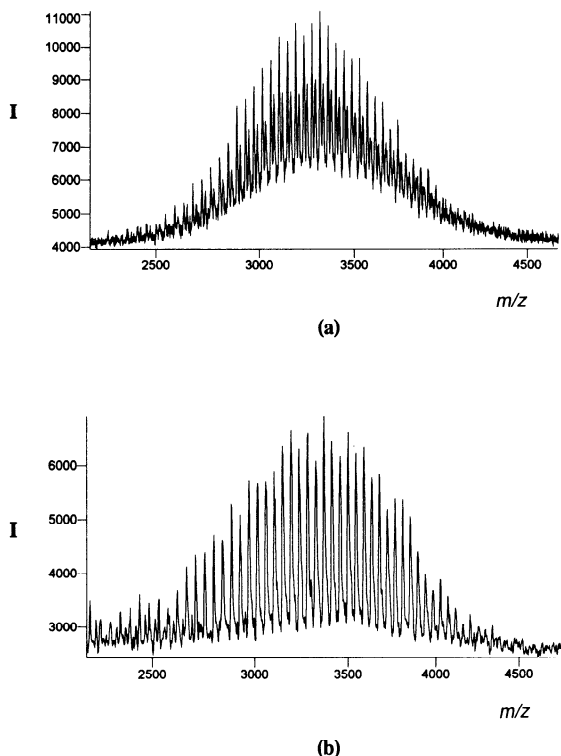


Figure 1. Positive-ion mass spectra of PEG 3300 in (a) IAA and (b) 9-ACA matrices. No alkaline salts were added.

$[M + Na]^+$, resulting in severe interferences (see Fig. 1(a)). The interference became more deleterious in the case of lower intensity peaks. Much better quality mass spectra were obtained in 9-ACA matrix showing all peaks baseline separated. The mass resolution was approximately 300 for each peak, compared to only 120 in IAA. In 9-ACA matrix, the absence of K^+ adducts also made some peaks on the fringe of the distribution (e.g. $m/z < 2500$ Da, and $m/z > 4000$ Da) discernible from noise.

Non-polar polymers are considered challenging analytes for MALDI-MS analysis. For these polymers, the low molecular weight fraction (below 1000 Da) is often readily cationized by metal ions, especially silver ion.¹⁷ We measured polybutadiene 1000 in 9-ACA matrix in the presence of Ag^+ . The peaks corresponding to $[M + Ag]^+$ ions of the oligomers were centered at a value corresponding to $M_w \approx 940$ Da, significantly lower than the weight-averaged molecular weight provided by the manufacturer ($M_w = 1000$ Da). Assuming that the polymer had been characterized by GPC, this observation fits the pattern of systematically lower average molecular weights observed by MALDI.¹⁴ For comparison, direct laser desorption with only Ag^+ as cationized reagent was performed for polybutadiene 1000. In this case, we obtained a group of polymer ion peaks centered at a value corresponding to $M_w \approx 841$ Da, a lower value than the one obtained in the presence of 9-ACA. These results indicated the possibility of metastable decay when only cationizing metal ion was added. The role of the matrix in this case could be construed as a 'cooling device' making the ionization process 'softer'. Larger non-polar polymers, e.g., PMMA 6000 were also tested. Results of these experiments are discussed in the Accelerating Voltage Effects section.

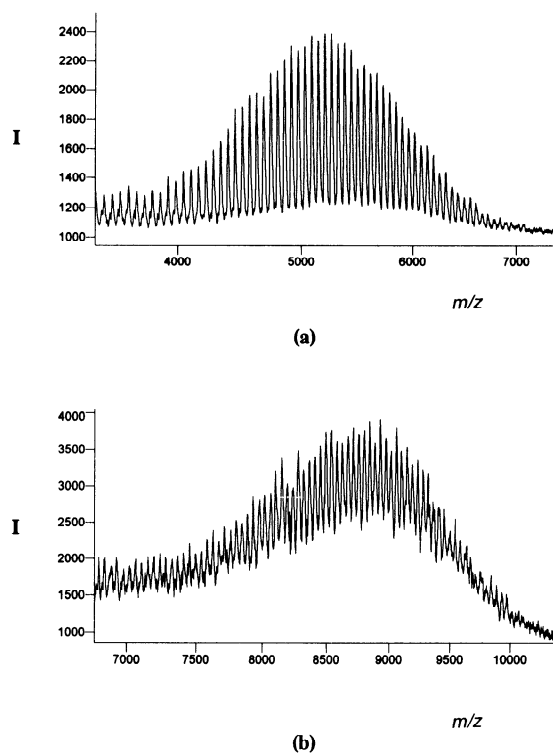


Figure 2. MALDI mass spectra of (a) PPG 5000 and (b) PEG 8000 using the 'super' 9-ACA matrix.

In addition to investigating the utility of the 9-ACA matrix, we also examined its binary mixtures of varying composition, focusing mostly on mixtures with 5-MSA, DHB, IAA, SA and sucrose. Superior results were acquired with 5:2 (molar ratio) mixture of 9-ACA and 5-MSA ('super' 9-ACA), especially for larger polymer molecules. The function of 5-MSA was thought to be to enhance ion desorption and reduce the internal energy of analyte ions.¹⁸ A number of PPGs and PEGs with average molecular weights between 450 and 15000 have been detected using 'super' 9-ACA. In Fig. 2 the mass spectra of PPG 5000 and PEG 8000 are displayed. Oligomer ions from Na^+ attachment were dominant for PPG 5000 with mass distribution of $M_n \approx 5195$ and $M_w \approx 5270$ (Fig. 2(a)). The mass resolution of 493 for m/z 5434 was sufficient to ascertain the absence of K^+ adducts. Although similar quality mass spectra could be obtained for PPG with M_w up to about 6000 Da in both 9-ACA and 'super' 9-ACA matrices, 'super' 9-ACA produced more abundant and more stable signal when heavier polymer fractions (>8000 Da) were measured. For example, a threefold increase in ion intensity was observed for PEG 8000 in 'super' 9-ACA compared to 9-ACA matrix.

Although the oligomer ion peaks of PEG 8000 could not be resolved completely due to the limitations of the linear TOF mass spectrometer, the mass of the repeat unit and the envelope of the molecular weight distribution were well defined. The oligomer distribution ranged from m/z 7477 to ca. 10500, corresponding to a degree of polymerization between $n = 169$ and ca. 238. In this case the weight-averaged molecular weight obtained by MALDI showed a positive discrepancy from the GPC data provided by the manufacturer. This observation conformed with the results reported in

another investigation.¹⁹ In both studies, MALDI-MS showed about 10% higher weight-average molecule weight for PEG 8000.

This observation points to the complexity of these discrepancies. Lehrle and Sarson explained the presence of *negative* discrepancies by lower desorption/ionization efficiency and/or more-pronounced decomposition of the larger oligomers during MALDI-MS.¹⁴ Their arguments, however, can not be applied to rationalize *positive* deviations from GPC data. GPC results can also present distortions, especially in the low-mass range where light-scattering detectors are less reliable. In addition, GPC separation is based on the hydrodynamic radius of polymer molecules and not on their molecular masses. Severe distortions of the oligomer size distributions may arise in GPC because of the dependence of retention times on polymer conformation (size effect) and on the nature of end groups.

Accelerating voltage effects

Distortions in the MALDI-MS of oligomer size distributions can be associated with every step of the sample preparation and measurement. The MALDI sample preparation involves dissolving the analyte, mixing the sample solution with matrix, and recrystallizing the mixture on the probe. Any of these steps may result in discrimination against certain oligomer fractions. Further distortion of the oligomer size distribution can occur during the desorption and ionization process. Laser irradiation of the sample can lead to analyte degradation on the probe tip, preferential desorption, preferential ionization, and selective metastable decay of certain ions. Additional discrimination may be attributed to instrumental effects. The extraction of ions by accelerating voltage, the transmission by the ion optics, and the response of the detector can all show different efficiencies for ions with different values of m/z . It was not our objective to differentiate between these factors in the present Communication.

Instead, we took a practical approach. We decided to explore the effect of accelerating voltage on the apparent oligomer size distribution of polymer standards. There are two major consequences of changing the accelerating voltage in a MALDI-MS experiment. Increased accelerating voltage leads to better ion extraction from the laser-generated plume and to higher detector sensitivity in the high-mass range. This latter effect is known to limit the observation of very heavy ions.

In order to see the influence of accelerating voltage on the detection of oligomer ions, three samples were examined: PPG 2000, PMMA 6000, and bovine insulin. At 30 kV accelerating voltage, strong sodiated ions were observed for PPG 2000 (mass spectra not shown). The obtained M_n , M_w , and M_p of 1965, 2172, and 2013 Da were in excellent agreement with the manufacturer's GPC data (1950, 2150, and 2000 Da for M_n , M_w , and M_p , respectively). When the accelerating voltage was lowered to 18 kV, the same number of oligomers was detected although the ion intensities decreased slightly and the mass resolution reduced from 300 to 170. For a higher mass polymer, PMMA 6000, the effects of accelerating voltage were much more significant. At 30 kV a well defined oligomer distribution was

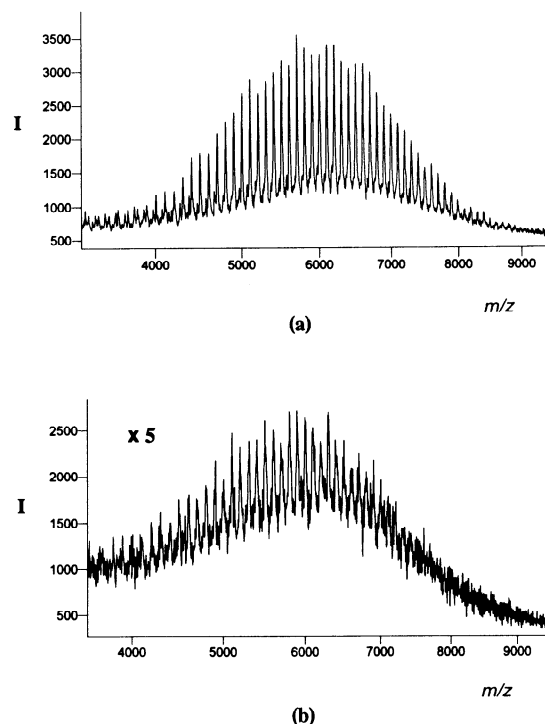


Figure 3. Polymer standard PMMA 6000 measured by MALDI-MS in 'super' 9-ACA matrix at (a) 30 kV; and (b) 18 kV accelerating voltages.

observed ranging from 3623 Da to 8523 Da (Fig. 3(a)). At 18 kV, however, we saw a very different picture (Fig. 3(b)). The ion intensity decreased by a factor of ~ 5 , the mass resolution dropped by a factor of 3.3, and the high-mass end of the spectrum was truncated, resulting in an apparent oligomer size distribution shift to lower mass. For example, M_n shifted from 6054 Da to 5775 Da and M_w moved from 6206 Da to 5844 Da (see Table 2). Similarly the molecular weight M_p , corresponding to the peak of the distribution, decreased from 6224 Da to 5923 Da. It was noted that in spite of the measured differences in molecular weight distributions, the calculated polydispersities at both accelerating voltages were similar (1.03 at 30 kV and 1.01 at 18 kV), but uniformly lower than those from the GPC data (1.08) provided by the manufacturer.

Table 2. Statistical analysis of oligomer size distributions measured by MALDI-MS and the corresponding values specified by the manufacturer for polymer standard PMMA 6000

	MALDI data		Manufacturer's data ^a
	30 kV ^b	18 kV ^b	
M_n	6054	5775	6000 (VPO), 6100 (GPC/DV)
M_w	6206	5844	6500 (GPC/DV)
M_p	6224	5923	6300 (GPC)
M_c^c	6061	5848	
$M/\Delta M^d$	400	120	
M_w/M_n	1.03	1.01	1.08
Skewness	-0.02	-0.21	
Kurtosis	-0.48	-0.53	

^a Results were based on GPC, vapor pressure osmometry (VPO), and GPC with differential viscometry (GPC/DV) measurements.

^b 30 kV and 18 kV refer to the accelerating voltage.

^c M_c is obtained as the center of the Gaussian fit to the oligomer size distribution (see Fig. 4).

^d Mass resolution calculated for the oligomer ion m/z 6023.

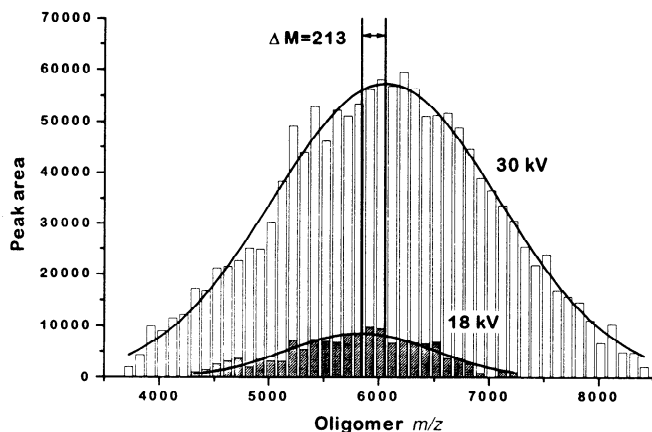


Figure 4. Comparison of observed peak areas and oligomer size distributions of PMMA 6000 at 30 kV and 18 kV accelerating voltages. The fitted Gaussian distributions indicate a substantial shift in the mean.

A detailed statistical analysis of the two distributions was based on the corresponding integrated ion current signal. Peak areas in the flight-time spectrum represented the total charge corresponding to individual oligomers. The distribution of peak areas at 18 kV and 30 kV is shown in Fig. 4. In order to describe the properties of the distributions the momenta (Eq. (3)) and the central momenta (Eq. (4)) were calculated. Table 2 shows the changes in skewness and kurtosis defined by Eqs. (8) and (9), respectively. When the accelerating voltage was lowered from 30 kV to 18 kV the skewness of the peak area distribution increased by a factor of ten. This substantial increase can also be seen intuitively by comparing the corresponding mass spectra (Figs 3(a) and (b)). No significant change was detected in the kurtosis values.

In Fig. 4 we also compared the fitted Gaussian distributions. While both the 30 kV and the 18 kV peak area could be approximated by bell curves, a significant change was observed in the center of the distribution (see the M_c values in Table 2). Lowering the accelerating voltage from 30 kV to 18 kV led to a calculated drop in M_c of $\Delta M = 213$ Da.

The substantial decrease in ion intensity at lower accelerating voltage was expected because the corresponding ion velocity was lower. According to Geno and Macfarlane the secondary electron emission coefficients for MCP are linear in mass and exponential in velocity.²⁰ For PMMA 6000 the oligomer ion signal at m/z above 7200 was not distinguishable from noise at 18 kV (Fig. 3(b)). If we assume that all ions enter the field-free region with the same kinetic energy, the ion velocity of m/z 7200 particles is about 2.2×10^4 m/s, in good agreement with the apparent threshold data of about 2×10^4 m/s.²⁰ For smaller polymer molecules, such as PPG 2000 oligomers, the detected signal did not change significantly because the ion velocities at both accelerating voltages ($\sim 5.3 \times 10^4$ for 30 kV and 3.8×10^4 m/s for 18 kV) were significantly higher than the apparent threshold velocity for the MCP detector. On the other hand, only the low mass fractions of PMMA 6000 had enough velocity to induce MCP detector response.

According to the calculations of Mamyrin *et al.*, in a linear TOF system where the accelerating region is

much shorter than the field-free region, the mass resolution can be expressed as:

$$\frac{M}{\Delta M} \approx \frac{eU}{E_0} \quad (10)$$

where U and E_0 refer to the accelerating voltage and the initial kinetic energy spread, respectively.²¹ There are three major sources of energy dispersion at the ion generation site: inherent energy differences due to the laser desorption, variations in the potential energy due to the location of ion generation, and energy changes due to collisions. Measuring the mass resolution for a given accelerating voltage, one can calculate the initial energy spread from Eq. (10). Due to the lower voltage, the mass resolution of insulin ions (5733.5 Da) in SA matrix decreased by only a factor of 2 (from 450 at 30 kV to about 230 at 18 kV) compared to a factor of 3.3 drop in the case of PMMA 6000 (Table 2). To explore the role of the three mentioned factors, we determined E_0 values for two similar size ions, insulin and a PMMA 6000 oligomer, at 30 kV and at 18 kV. Insulin ions desorbed from SA matrix with $E_0 \approx 67$ eV, whereas the PMMA 6000 ions left the 'super' 9-ACA host with $E_0 \approx 75$ eV. At 18 kV, however, the initial energy spread doubled for PMMA 6000 ($E_0 \approx 150$ eV), whereas only a 16% increase was observed for insulin ($E_0 \approx 78$ eV).

During our experiments with a particular matrix, the laser irradiance was kept constant; thus, we assumed that the inherent kinetic energies of analyte ions were similar at different accelerating voltages. Lowering the accelerating voltage would have decreased the energy spread if it was associated with the location of ion generation. In contrast, the mechanism based on the collisional energy exchange could account for the increasing energy spread at lower voltages. At 18 kV the ions spent more time in the relatively high density environment of the accelerating region, resulting in a larger number of collisions. In the case of oligomer ions, these collisions took place not only with small matrix-related particles but also with other oligomers similar in size. Thus collision-induced kinetic energy spread was expected to be more important for similarly sized oligomers than for individual proteins. Our observations were consistent with this picture.

Acknowledgements

The authors are indebted to the National Science Foundation for the financial support (Grant No. CTS-9212389) to purchase the excimer laser and part of the dye-laser system. We also thank the George Washington University for providing funds to acquire the second-harmonic generator and the laser coupling optics. The polymer standard samples were kindly supplied by W. R. Grace & Co.-Conn. Partial support for one of the authors (X.T.) by the George Washington University Facilitating Fund and W. R. Grace & Co.-Conn. is also gratefully acknowledged.

REFERENCES

1. A. Vertes and R. Gijbels, in *Laser Ionization Mass Analysis*, A. Vertes, R. Gijbels and F. Adams (Eds), John Wiley & Sons, New York, 1993, p. 127.
2. U. Bahr, A. Deppe, M. Karas and F. Hillenkamp, *Anal. Chem.* **64**, 2866 (1992).
3. P. O. Danis, D. E. Karr, F. Mayer, A. Holle and C. H. Watson, *Org. Mass Spectrom.* **27**, 283 (1992).
4. X. Xiong and K. G. Owens, *Proc. 42nd Conf. on Mass Spectrometry and Allied Topics*, Chicago, 1994, p. 980.
5. R. C. King and K. G. Owens, *Proc. 42nd Conf. on Mass*

- Spectrometry and Allied Topics*, Chicago, 1994, p. 955.
6. P. O. Danis, D. E. Karr, D. Westmoreland, M. C. Piton, D. I. Christie, P. A. Clay, S. H. Kable and R. G. Gilbert, *Macromolecules*, **26**, 6684 (1993).
 7. K. Strupert, M. Karas and F. Hillenkamp, *Int. J. Mass Spec. Ion Processes* **111**, 89 (1991).
 8. P. O. Danis and D. E. Karr, *Org. Mass Spectrom.* **28**, 923 (1993).
 9. G. Montaudo, M. S. Montaudo, C. Puglisi and F. Samperi, *Rapid Commun. Mass Spectrom.* **8**, 1011 (1994).
 10. F. Xiang and R. C. Beavis, *Rapid Commun. Mass Spectrom.* **8**, 199 (1994).
 11. J. H. Callahan, unpublished results.
 12. J. Zhou and T. D. Lee, *Proc. 43rd Conf. on Mass Spectrometry and Allied Topics*, Atlanta, 1995.
 13. G. B. Hurst, T. J. Czartoski and M. V. Buchanan, *Proc. 42nd Conf. on Mass Spectrometry and Allied Topics*, Chicago, 1995, p. 975.
 14. R. S. Lehrle and D. S. Sarson, *Rapid Commun. Mass Spectrom.* **9**, 91 (1995).
 15. Z. Olumee, M. Sadeghi, X. Tang and A. Vertes, *Rapid Commun. Mass Spectrom.* **9**, 744 (1995).
 16. X. Tang, A. Vertes, P. A. Dreifuss, C. Hull and W. Dutton, *Proc. 43rd Conf. on Mass Spectrometry and Allied Topics*, Atlanta, 1995.
 17. M. S. Kahr and C. L. Wilkins, *J. Am. Soc. Mass Spectrom.* **4**, 453 (1993).
 18. A. Tsarbopoulos, M. Karas, K. Strupat, B. N. Pramanik, T. L. Nagabhushan and F. Hillenkamp, *Anal. Chem.* **66**, 2062 (1994).
 19. M. Dey, J. A. Castoro and C. L. Wilkins, *Anal. Chem.* **67**, 1575 (1995).
 20. P. W. Geno and R. D. Macfarlane, *Int. J. Mass Spectrom. Ion Processes* **92**, 195 (1989).
 21. B. A. Mamyrin, V. I. Karataev, D. V. Shmikk and V. A. Zagulin, *Soviet Phys. JETP* **37**, 45 (1973).